The Prostate

WILEY

The Prostate

ORIGINAL ARTICLE OPEN ACCESS

PRMT5:MEP50 Are Mediators of Treatment-Induced Neuroendocrine Differentiation in Prostate Cancer

Hye Seung Nam[1] | Andrew Michael Asberry[1] | Xuehong Deng[1] | Sheng Liu[2,3] | Jiaoti Huang[4] | Chang-Deng Hu[1,5] | Jun Wan[2,3,6] | Michael K. Wendt[1,5]

[1]Borch Department of Medicinal Chemistry and Molecular Pharmacology, Purdue University, West Lafayette, Indiana, USA | [2]Department of Medical and Molecular Genetics, Indiana University School of Medicine, Indianapolis, Indiana, USA | [3]Indiana University Simon Comprehensive Cancer Center, Indiana University School of Medicine, Indianapolis, Indiana, USA | [4]Department of Pathology, Duke University School of Medicine, Duke University, Durham, North Carolina, USA | [5]Purdue Institute for Cancer Research, Purdue University, West Lafayette, Indiana, USA | [6]Center for Computational Biology and Bioinformatics, Indiana University School of Medicine, Indianapolis, Indiana, USA

Correspondence: Michael K. Wendt (mwendt@purdue.edu)

Received: 5 March 2025 | **Revised:** 21 May 2025 | **Accepted:** 23 June 2025

Funding: This study was supported by Purdue University Center for Cancer Research and DOD Prostate Cancer Research Program.

Keywords: drug resistance | enzalutamide | neuroendocrine | PRMT5

ABSTRACT

Background: Neuroendocrine prostate cancer (NEPC) is a lethal subtype of prostate cancer responsible for an estimated 20%–30% of castration-resistant prostate cancer (CRPC) deaths. While NEPC can arise spontaneously, the majority of these cases emerge as treatment-induced NEPC (tNEPC). Our clinical and computational analyses identified increased expression of protein methyltransferase 5 (PRMT5) and its cofactor methylosome protein 50 (MEP50) in tNEPC.

Methods: Here we generated an in vitro cell culture and mouse model of prostate cancer to recapitulate tNEPC induced upon treatment with the androgen receptor (AR) inhibitor, enzalutamide. The role of PRMT5 and its cofactor MEP50 were determined by overexpression. Depletion of these genes and pharmacological inhibition of PRMT5 were followed by analysis of cell viability, neurite growth, and effects on neuroendocrine-related gene transcription using immunofluorescence, immunohistochemistry, and Western blot. PRMT5 and MEP50 protein expression levels were comprehensively analyzed for clinical correlation in NEPC patient prostate tissue samples.

Results: Elevated PRMT5 and MEP50 correlated with increased recurrence in prostate cancer patients receiving androgen deprivation therapy. Depletion of PRMT5 and MEP50 prevented neuroendocrine differentiation (NED)-induced by enzalutamide both in vitro and in a xenograft mouse model. Conversely, overexpression of PRMT5 and MEP50 was sufficient to induce NED in prostate cancer cells. Evaluation of a genetically engineered mouse model, in which PRMT5 and MEP50 were overexpressed in the prostate, similarly indicated NEPC development.

Conclusions: Our data suggest that PRMT5:MEP50 are regulators of tNEPC. PRMT5/MEP50 expression could serve as a predictive biomarker and therapeutic target for aggressive forms of prostate cancer.

1 | Introduction

Over the last decade, advances in targeting androgen receptor (AR) signaling have improved outcomes for prostate cancer patients [1–4]. Potent AR inhibitors such as enzalutamide (ENZ) have become first-line therapy for prostate cancer patients [5]. While these therapies are initially efficacious, 17%–30% of patients will progress to treatment-induced neuroendocrine prostate cancer (tNEPC), the most lethal histological subtype of prostate cancer [6]. Through the processes of neuroendocrine differentiation (NED), AR-dependent luminal epithelial cells differentiate into AR-independent basal-like cells [7]. Markers of NED include enhanced expression of chromogranin A (CgA), synaptophysin (SYP), and neuron-specific enolase (NSE) [8].

Accumulating evidence shows that NED is largely regulated through epigenetic processes that control transcriptional reprogramming [9]. Epigenetic reprogramming includes the action of multiple transcription factors, histone modifications, and alteration of DNA methylation [10–12]. Other reports indicate that neuronal transcription factors such as achaete-scute family bHLH transcription factor 1 (ASCL1) and neuronal differentiation 1 (NEUROD1) can drive NED in CRPC cells. ASCL1 increases H3K27me3 levels through regulating EZH2 activity [13]. Similarly, master neuronal transcription factors such as BRN2 and SOX2 can regulate the global epigenetic landscape via histone 3 hypomethylation of prostate cancer cells to induce NED [14, 15]. Together, these findings highlight the importance of understanding the function of epigenetic modifiers in prostate cancer cells undergoing NED.

Protein arginine methylation is a key posttranslational modification with roles in maintaining cell homeostasis and disease phenotype. Protein arginine methyltransferase-5 (PRMT5) is classified as a type II protein arginine methyltransferease that symmetrically dimethylates arginine residues of histones and non-histone substrates [16]. By interacting with the N-terminal region of PRMT5 to create a heterooctameric complex, methylosome protein 50 (MEP50) serves as a crucial PRMT5 cofactor that aids in substrate recognition and placement [17]. Since MEP50 increases PRMT5 activity towards SmD3 protein, MEP50 may interact to change substrate specificity or activate PRMT5 methyltransferase activity [18]. In fact, we have previously reported that PRMT5 alongside with its cofactor MEP50 mediates chemotherapy-induced neuroendocrine differentiation in non-small cell lung cancer (NSCLC) [19]. Additionally, we previously reported that PRMT5 is overexpressed in high-grade tumors of prostate cancer and that its expression correlates with the expression of AR [20–22]. PRMT5 can localize to the AR promoter and methylate H4R3 to promote AR transcription [20, 23, 24]. Furthermore, we have also demonstrated that PRMT5 expression is essential for the repair of DNA double-strand break (DSB) and thus can sensitize prostate cancer cells to radiation and chemotherapy [25]. PRMT5 can also regulate the expression and activity of MYCN [26], p53 [27, 28], PTEN [29], and Rb [30]. These mechanistic studies clearly point to a role of PRMT5 in driving therapeutic resistance and prostate cancer progression.

In the present study, we demonstrate that PRMT5, when in conjunction with the cofactor MEP50, regulates tNEPC initiation and disease progression. Our in vitro and in vivo studies provide insights into the role of PRMT5:MEP50 in NED.

2 | Materials and Methods

2.1 | Cell Culture and Reagents

The LNCaP, C4-2, and NCI-H660 cell lines were purchased from ATCC. Cells were stored as frozen stock in the vapor phase of LN2 and thawed before use. Cell lines were cultured in three passages after thawing before experimentation and maintained for no longer than 30 total passages. LNCaP cells were cultured in RPMI 1640 (Corning) supplemented with 10% FBS (Atlanta Biologicals), 1 mM sodium pyruvate (Corning), penicillin (100 units/mL) and streptomycin (100 μg/mL) combination (Gibco), and 2 mM/L L-glutamine (Corning). C4-2 cells were cultured in DMEM/F12 (Gibco) supplemented with 10% FBS (Atlanta Biologicals), 0.100 μg/mL insulin (Sigma-Aldrich), 275 ng/mL triiodothyronine (Sigma-Aldrich), 88.6 ng/mL apo-Transferrin (Sigma-Aldrich), 4.9 ng/mL d–Biotin (Sigma-Aldrich), 251.8 ng/mL Adenine (Sigma-Aldrich), and penicillin (100 units/mL) and streptomycin (100 μg/mL) combination (Gibco). NCI-H660 cell lines were cultured in HITES media, formulated as follows: RPMI-1640 (Corning), 5% FBS (Atlanta Biologicals), 10 nM hydrocortisone (Sigma-Aldrich), 10 nM β-estradiol (Sigma-Aldrich), 1× Insulin-Transferrin-Selenium (Gibco), and 2 mM/L L-glutamine (Corning). For NED induction, cells were seeded at 80,000 cells per 6-well culture dish and allowed to attach to the dish overnight before enzalutamide treatment. Enzalutamide was purchased from MedchemExpress.

2.2 | Cell Transfection

LNCaP cells were seeded in 6 cm culture plates to be confluent on the following day, with 3 mL medium in each well, and then incubated in a CO_2 incubator overnight. Plasmid DNA and FuGENE HD Reagent (Promega) in a 1:3 weight ratio were mixed with 500 μL of OPTMEM, and the mixture was incubated for 20 min at room temperature. Finally, the mixture was dropped into each well and incubated in the CO_2 incubator.

2.3 | Morphological Analysis

Percent of NED induction was calculated morphologically from brightfield images acquired on the day as specified by observation. Images were acquired on a Nikon TE2000-U microscope with a 10× objective. Images were analyzed with ImageJ. NE-like cells were defined as cells with neurite extensions longer than twice the length of the cell body as described.

2.4 | Microscopic Observation

For cellular images in Figure 3, cultured LNCaP cells were directly observed under an Olympus 60-fold objective lens microscope (Nikon). Fluorescence images were observed using the GFP filter cube. Percent of NED induction was calculated as described in Section 2.3 from GFP images.

2.5 | Western Blot Analysis

Cells were lysed in RIPA buffer for 1 h on ice. Cell lysates were centrifuged at 12,000g for 20 min at 4°C, then 5× SDS sampling buffer (100 mM Tris-HCl pH 6.8, 4% SDS and 20% glycerol with bromophenol blue) was added and boiled at 95°C for 5 min. The proteins were separated through 10% SDS-PAGE gels and were transferred to a nitrocellulose membrane using Trans-Blot SD wet transfer cell (Bio-Rad). The membrane was blocked in 5%

nonfat dry milk-PBS for 2 h, washed, and incubated with primary antibodies in PBS containing 0.1% Tween 20 (PBST) overnight in agitation at 4°C. Unbound primary antibodies were removed by washing the membrane three times in PBST. The membrane was then incubated with a secondary antibody for 1 h at RT. After three washes with PBST, membranes were visualized with Odyssey XF Imaging System. The intensity of bands was determined with Image Lab software (Bio-Rad, Hercules, CA, USA). Antibodies against AR (1:2000, Cell Signaling), ARV7 (1:1000, Abcam), CgA (1:5000, Abcam), NSE (1:2000, Genetex), ASCL1 (1:1000, LS-Bio), NCAM1 (1:1000, Genetex), β-actin (1:5000, Sigma-Aldrich), and LI-COR IRDye 800CW Goat anti-Rabbit IgG (H + L), 0.5 mg (1:20000, LI-COR) and LI-COR IRDye 800CW Goat anti-Mouse IgG (H + L), 0.5 mg (1:20000, LI-COR) were used for Western blot analysis probing.

2.6 | Immunohistochemistry Analysis

Mouse genital urothelial tissues were collected and fixed in 10% formalin and paraffin-embedded following with H&E staining and immunohistochemical (IHC) staining. Antibodies against NSE (1:100, GTX, N1C1), CgA (1:100, Abcam, ab45179), Ki-67 (1:100, Cell Signaling Technology, 9449), or Myc (1:100, Abcam, ab32) were applied on sections overnight in 5% nonfat dry milk in PBS. After three washes in PBS, sections were probed with corresponding secondary HRP-conjugated antibodies diluted (1:100) in 5% nonfat dry milk in PBS for 1 h at room temperature. Sections were incubated with diaminobenzidine for 10 min and then counterstained with H&E. Image analysis and quantification were performed using Fiji software.

2.7 | Animal Models

All procedures were conducted in accordance with the Purdue University Animal Care and Use Committee. The coding sequences for Myc tag PRMT5 (Myc-PRMT5) and Myc tag MEP50 (Myc-MEP50) were cloned into the pBlueScript II SK (+)-ARR2PB-Intron-bGHPolyA plasmid using NheI and EcoRV restriction sites for Myc-PRMT5 and BmtI and EagI for Myc-MEP50. Androgen-dependent expression of the transgenes was independently validated in LNCaP cells via Fugene HD (Promega, Madison, WI, USA)-mediated plasmid transfection, both in the presence and absence of R1881, a synthetic androgen analog. Transgenic mice were generated using the C57BL/6N strain at the Purdue Transgenic Mouse Core Facility. Founders were identified by PCR screening of tail-tip DNA, utilizing specific primer pairs for PRMT5 (PRMT5-bGH-Fw and PRMT5-bGH-Rv, 312 bp product) and MEP50 (MEP50-bGH-Fw and MEP50-bGH-Rv, 332 bp product), along with T Cell Receptor (TCR) alpha -Fw and TCR-Rv primers (206 bp product) as an internal PCR control. Primer sets to identify PRMT5 are 5′-TCTGCTATTCATAACCCCACAGGC-3′ and 5′-GCCTGCTATTGTCTTCCCAATCCTC-3′, MEP50 are 5′- TGGTGTTCTCCCCACACAGTGTTCC-3′ and 5′-CAACTAGA AGGCACAGTCGAGGCTGA-3′, and TCR are 5′-CAAATGTTGC TTGTCTGGTG-3′ and 5′-GTCAGTCGAGTGCACAGTTT-3′. Male transgenic founders were mated with wild-type (WT) C57BL/6N females to confirm the inheritance of transgenes across at least three generations. Once transgene stability was established, PB-PRMT5 and PB-MEP50 mice were interbred to produce cohorts of double-transgenic (PB-PRMT5; PB-MEP50), single-transgenic (PB-PRMT5 or PB-MEP50), and WT mice for further studies.

2.8 | MTS Cell Growth Assay

NCI-H660 cells were diluted to 5000 cells/well in 100 μL/well culture medium into 96-well plates. Cells were incubated for 24 h at 37°C and 5% CO_2. Twenty microlitres per well of CellTiter 96 AQueous One Solution Reagent (Promega) was added to each well. Plates were incubated at 37°C and 5% CO_2 for 3 h. Absorbance at 490 nm using a 96-well plate reader. Absorbance readings from blank, culture medium without cells, were subtracted from each reading and normalized to the control (DMSO-treated).

2.9 | Statistical Analysis

Statistical analysis was performed using GraphPad PRISM software. For western blot, data were analyzed using a student *t*-test.

3 | Results

3.1 | PRMT5 and MEP50 Are Upregulated in Aggressive Prostate Cancer

We first sought to establish the relationship between PRMT5 and MEP50 (WDR77) in aggressive subtypes of prostate cancer. We found that expression between PRMT5 and MEP50 were positively correlated in high Gleason-score prostate cancer patients (Figure 1A). PRMT5 mRNA expression was also positively correlated with MEP50 mRNA expression in neuroendocrine prostate cancers (Figure 1B). Overall patient survival rate was significantly decreased as a function of PRMT5 or MEP50 expression (Figure 1C,D). Similar to mRNA levels, increased expression and correlation of PRMT5 and MEP50 at the protein level were observed in NEPC patient tissue samples when compared to localized or benign lesions (Figure 1E–G). Taken together, these data suggest dual expression of PRMT5 and MEP50 is associated with more aggressive subtypes of prostate cancer.

3.2 | Suppression of PRMT5:MEP50 Reduces Treatment-Induced NED and Resensitizes Cells to Inhibition of Androgen Receptor

We next sought to investigate the functional role of PRMT5 and MEP50 in NED. Therefore, we depleted PRMT5 in the C4-2 cell line in a doxycycline-inducible manner as previously reported (Figure 2A) [24]. Depletion of PRMT5 inhibited ENZ-induced neurite outgrowth and increased cell death in these treatment-resistant prostate cancer cells (Figure 2B,C, Figure S1A–D). Similarly, depletion of MEP50 also inhibited NED and increased cell death induced by either ENZ (Figure S1A-D) or androgen deprivation, through the use of charcoal/dextran-stripped fetal bovine serum (CDS-FBS) (Figure 2D–F). Genetic depletion of

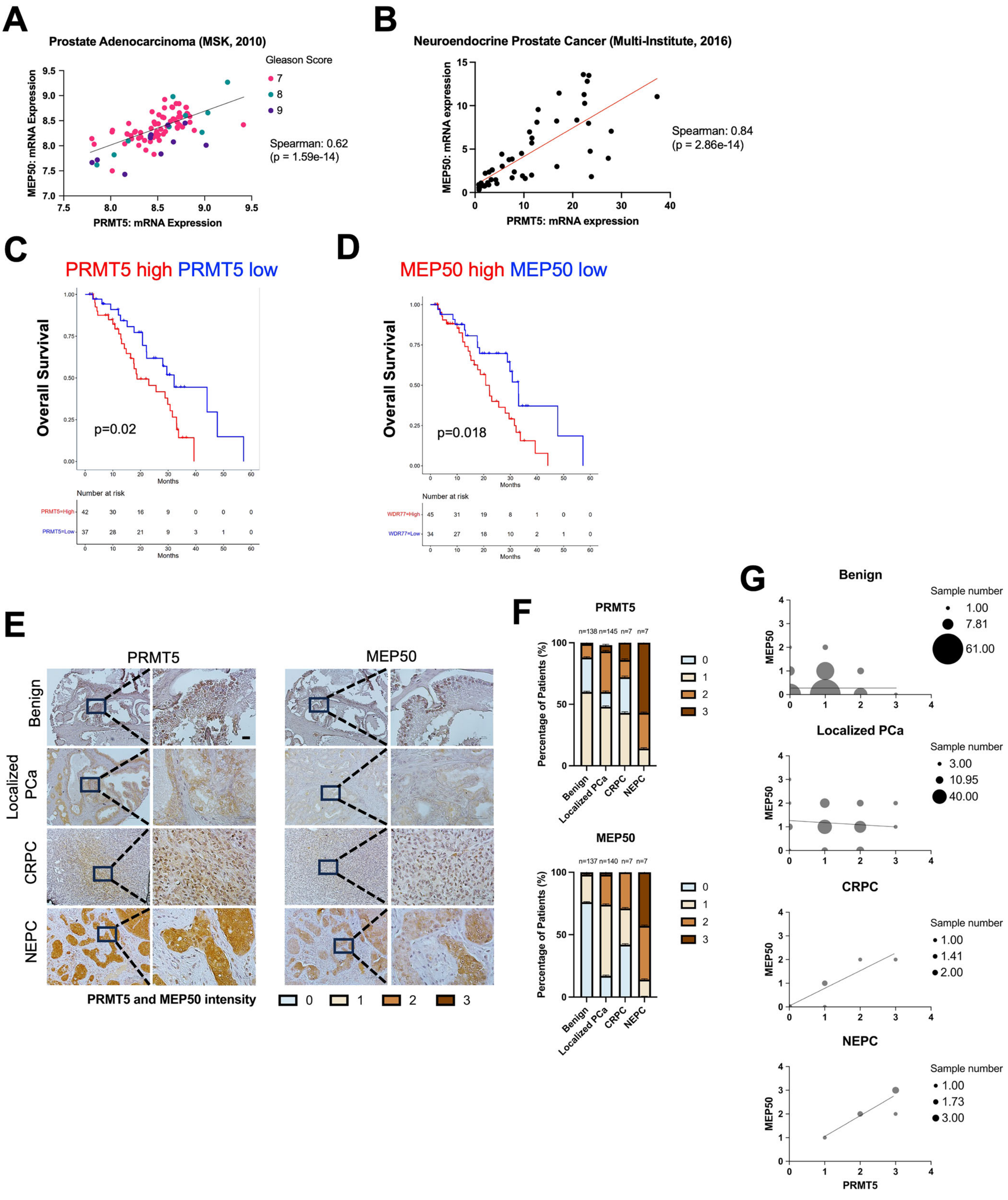

FIGURE 1 | PRMT5 and MEP50 are upregulated in aggressive prostate cancer. (A) Scatter plot showing the correlation of PRMT5 and MEP50 mRNA expression in groups of patients with indicated Gleason scores. Patient data was filtered to include only those individuals who underwent radical prostatectomy. Data were analyzed using linear regression, yielding the indicated Spearman *r* and *p*-value. (B) Correlation of PRMT5 and MEP50 expression were similarly compared in neuroendocrine prostate cancer patients. (C and D) Kaplan–Meier survival curves comparing overall patient survival based on PRMT5 or MEP50 (WDR77) expression. (E) Representative images of benign, localized prostate cancer, CRPC and NEPC patient tissue samples stained for CgA, PRMT5, and MEP50. (F) Quantification of PRMT5 and MEP50 expression intensities plotted across disease stage as shown in panel E. (G) Correlation of PRMT5 and MEP50 expression across disease stages shown in panel E. For panels F and G IHC staining intensity was determined using Fiji software. Results are mean ± SD from three independent experiments, and multiple *t*-test was used for *p*-value determination. [Color figure can be viewed at wileyonlinelibrary.com]

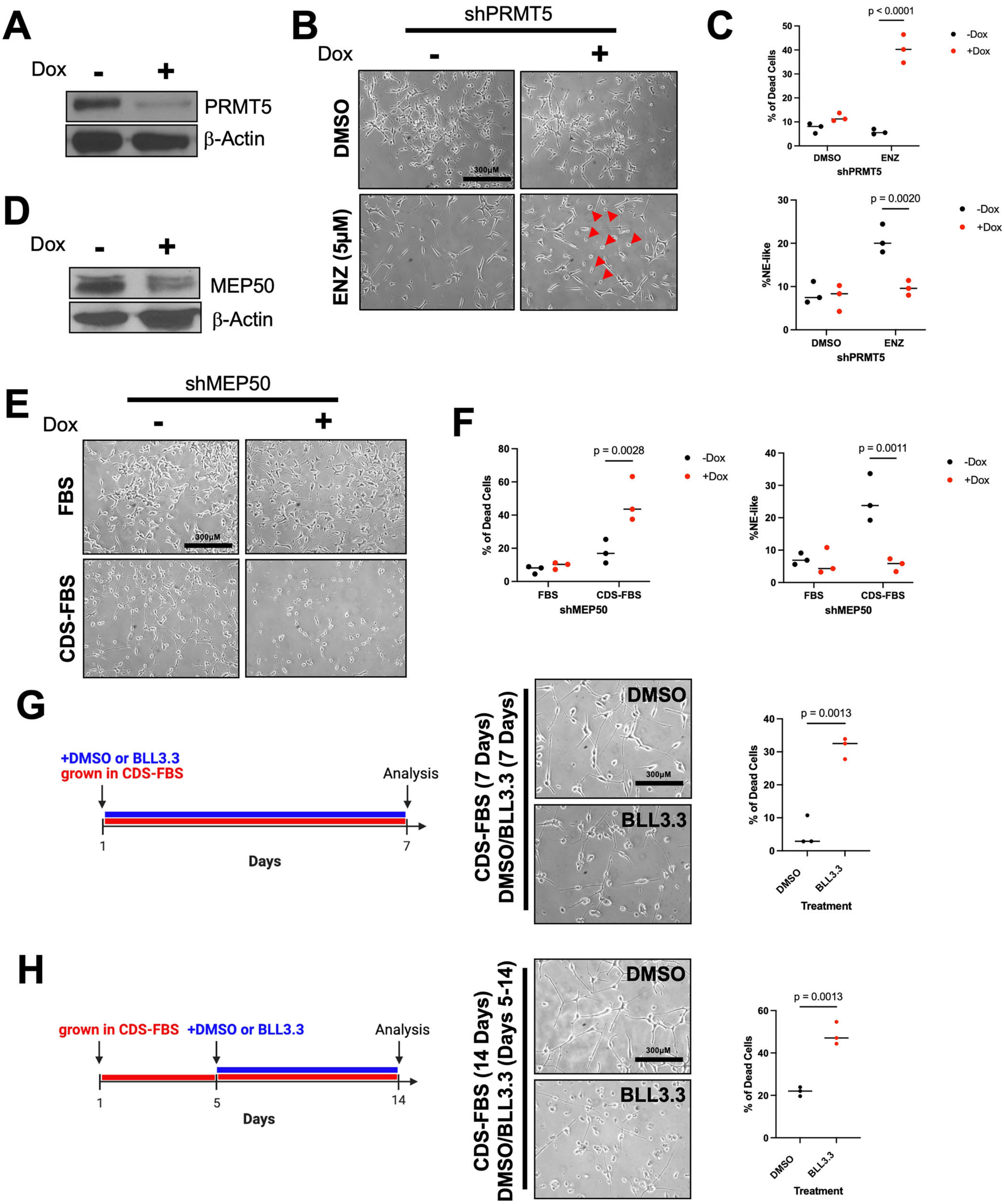

FIGURE 2 | Legend on next page.

PRMT5 and MEP50 under DMSO-treated or complete media conditions did not show any changes in cell death or NED (Figure 2C,F).

Next, we utilized the NCI-H660 cells, an NEPC cell line derived from a patient tumor biopsy. These cells were treated with either DMSO or the PRMT5 inhibitor, BLL3.3 [22, 24]. Similar to our shRNA approaches, BLL3.3 induced cell death and cell growth inhibition (Figure S2A–C). Furthermore, the expression of the NED markers, CgA and NSE were also downregulated by BLL3.3 treatment (Figure S2D,E). In contrast, BLL3.3 did not affect the viability of the non-NEPC, LNCaP cell line (Figure S2F,G).

3.3 | PRMT5 and MEP50 Are Necessary and Sufficient to Induce NED In Vitro

To further scrutinize the functional role of PRMT5:MEP50 in NED, we independently or co-expressed PRMT5 and MEP50 in LNCaP cells and quantified extended neurite outgrowth (Figure 3A). For this approach, we utilized our GFP overexpressing LNCaP cell line, which offers high sensitivity for detecting changes in cell morphology. Co-expression of both PRMT5 and MEP50 initiated NED, with 30% of cells exhibiting neurite extension outgrowth compared to 11% from vector control (Figure 3B). In contrast to wild-type proteins, co-expression of a catalytically inactive PRMT5 (R368A) with MEP50 failed to induce extended neurite outgrowth (Figure 3C,D) [31]. Similarly, co-expression of PRMT5 with a MEP50 mutant (D99A) that is unable to interact with PRMT5 also did not induce extended neurite formation (Figure 3C,D) [32]. Consistent with these morphological changes, expression of NED-marker proteins, CgA and NCAM1, were also significantly induced upon co-expression of wild type PRMT5/MEP50, but not the interaction-deficient mutants (Figure 3E–G, Figure S3A,B). These findings suggest that co-expression of PRMT5 and MEP50 is sufficient to induce NED in LNCaP cells. PRMT5 has additional co-factors, such as pICln and RIOK1 [17]. Therefore, we evaluated the impact of PRMT5 overexpression with either pICln or RioK1 on NED (Figure S3C). In contrast to MEP50, expression of pICln nor RIOK1 did not induce CgA expression (Supplementary Figure 3C,D). These data together with those from Figure 2, suggest that the formation of a catalytically active PRMT5/MEP50 complexes are necessary and sufficient for the induction of NED in LNCaP cells.

3.4 | PRMT5 and MEP50 Can Initiate and Regulate NED Induction In Vivo

To define the role of PRMT5:MEP50 during in vivo initiation of NED in prostate adenocarcinoma, we expressed PRMT5 and MEP50 in the mouse prostate under control of the probasin (PB) promoter. We first generated the PB-PRMT5 and PB-MEP50 mouse model and crossbred them to develop PB-PRMT5/PB-MEP50 mice. Animals expressing Myc-tagged PRMT5 and MEP50 alone or together were evaluated for induction of NED in the genital and urinary (GU) organs (Figure 4A). At 52 weeks of age IHC staining was performed on GU tissues to monitor for confirmation and degree of PRMT5 and MEP50 overexpression and disease progression. Animals expressing both PRMT5 and MEP50 had the highest proliferative index (Figure 4B). This hyperplasia was consistent with the induction of mouse prostatic intraepithelial neoplasia (mPIN) and invasive adenocarcinoma in different lobes of the prostate (Figure 4C). Furthermore, more aggressive pathology was observed in PRMT5:MEP50 expressing tumors (Figure 4D). Finally, PRMT5:MEP50 expressing mice had significantly enhanced expression of the NED markers NCAM1 and ASCL1 (Figure 4E,F). These analyses indicate that combined expression of PRMT5:MEP50 in murine prostate epithelium is sufficient to drive NEPC.

3.5 | Perturbation of PRMT5 Expression Inhibits Treatment-Induced NED In Vivo

To further expand our findings, we analyzed our previously reported PRMT5 knockdown (KD) 22rv1 xenograft mouse model (Figure 5A) [24]. Treatment of control 22rv1 tumors with enzalutamide failed to reduce proliferation (Figure 5B,C). However, enzalutamide treatment did enhance expression of NED markers, NCAM1 and ASCL1 (Figure 5D,E and Figure S4A). Depletion of PRMT5 sensitized these resistant tumor cells to enzalutamide, resulting in a significant reduction in Ki67 index and reduced ASCL1 and NCAM1 expression (Figure 5D,E and Figure S4A). MEP50 expression remained unchanged upon either PRMT5 depletion or enzalutamide treatment (Figure S4B,C). Taken together, these findings suggest that targeting PRMT5 can reduce treatment-induced NED and sensitize tumors to enzalutamide.

FIGURE 2 | Depletion of PRMT5:MEP50 reduces treatment-induced NED and resensitizes cells to inhibition of androgen receptor. (A) Immunoblot analyses for PRMT5 in C4-2 cells expressing doxycycline (Dox) inducible shRNAs targeting PRMT5 (shPRMT5). Cells were treated with Dox (1 μg/mL) for 7 days before analysis. Assessment of β-Actin served as a loading control. (B) The cells described in panel A were treated with either DMSO or enzalutamide (ENZ) as indicated. Red arrows indicate dead cells. (C) Cell death was determined using Trypan blue staining and NE-like cells were determined by the two times longer neurites than cell body diameter. Data in panel C represent the quantified number of NE-like cells and cell death from panel B images. (D–F) PRMT5 expression was depleted by Dox-inducible shRNAs in LNCaP cells. These cells were cultured in full media (FBS) or induced to undergo NED by CDS-FBS for 7 days with MEP50 gene downregulation (Dox +) or without gene downregulation (Dox-). (D) Cells were treated with Dox (1 μg/mL) for 7 days before immunoblot analysis for PRMT5. Assessment of Actin served as a loading control. (E) The cells described in panel D were grown in CDS-FBS media for 7 days. (F) The percentage of cell death and NE-like cells were quantified. (G) Left schematic diagram shows the experimental time course. LNCaP cells were grown under CDS-FBS in the presence of either 10 μM of the PRMT5 inhibitor BLL3.3 or DMSO for 7 days. Cells were imaged by phase contrast microscopy (150×) and percent cell death was quantified. (H) Left schematic diagram shows the experimental time course. LNCaP cells were first grown under CDS-FBS for 5 days to induce NED. Cells were subsequently maintained by CDS-FBS for an additional 9 days in the presence of BLL3.3 or DMSO. Cells were imaged by phase contrast microscopy (150×) and percent cell death was quantified. Results are mean ± SD from three independent experiments, and multiple *t*-test was used for *p*-value determination. [Color figure can be viewed at wileyonlinelibrary.com]

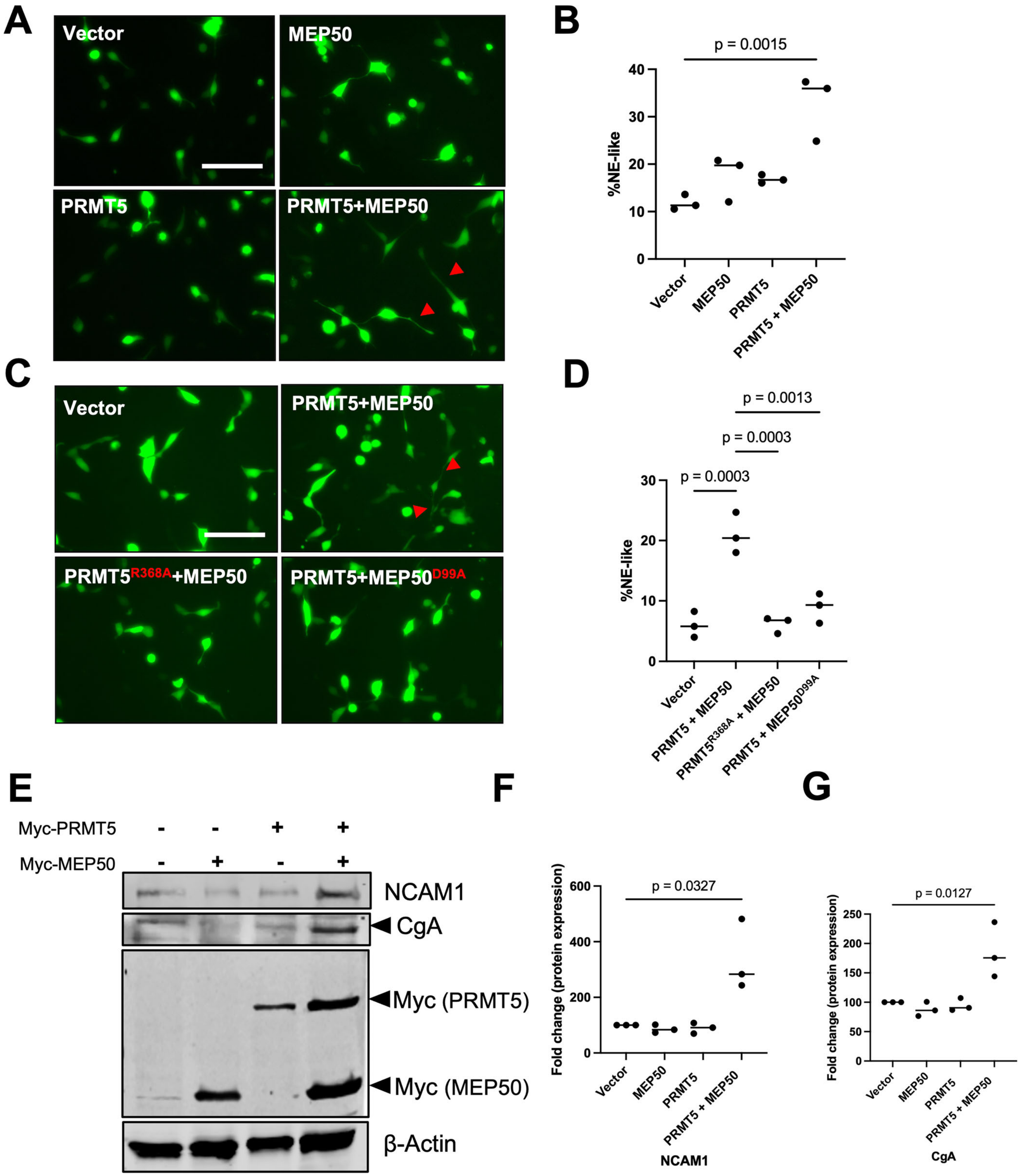

FIGURE 3 | PRMT5 and MEP50 are necessary and sufficient to induce NED in vitro. (A) Shown are representative images acquired 72 h after transient transfection of LNCaP cells with pMyc-PRMT5 or pMyc-MEP50 expressing plasmids. Red arrows indicate extended neurite growth. (B) Quantified NE-like cells from experiments in A. (C) Expression of a catalytic inactive mutant PRMT5 (R368A) or PRMT5 interaction defective MEP50 (D99A) failed to induce extended neurite outgrowth in LNCaP cells. (D) Quantified NE-like cells from experiments in C. (E) Representative immunoblotting from experimental conditions described in panel A. (F and G) Densitometry analyses for NCAM1 and CgA from 3 independent experiments. Band intensities were quantified by ImageStudio and normalized to Actin. Results are mean ± SD from three independent experiments, and multiple *t*-test was used for *p*-value determination. [Color figure can be viewed at wileyonlinelibrary.com]

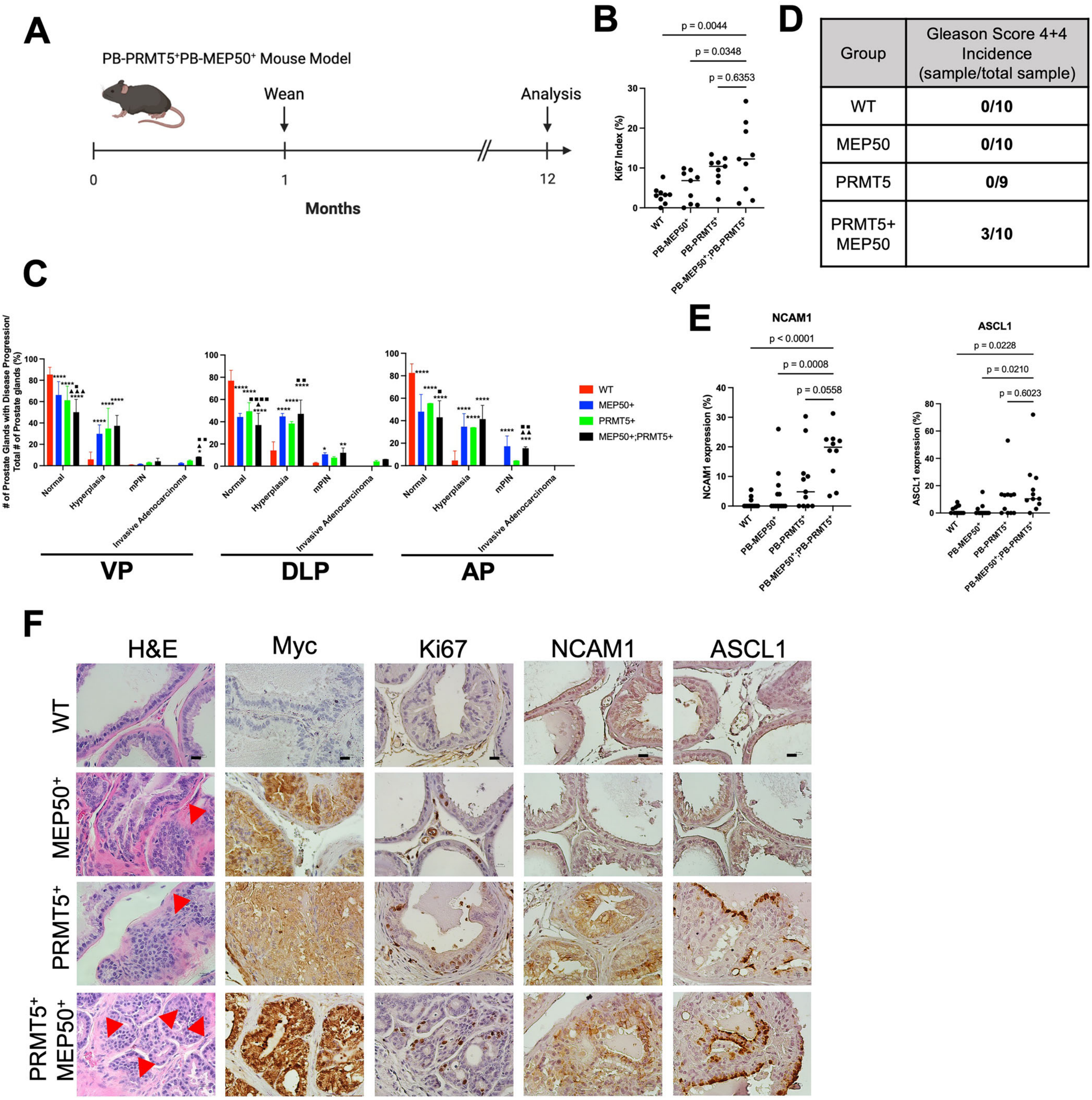

FIGURE 4 | PRMT5 and MEP50 can initiate and regulate *in vivo* NED induction. (A) Schematic plan of mouse studies. Created with Biorender.com. Figures (B) Ki67 index from prostates of mice of the indicated genotype. (C) Bar graph representing the number of prostate glands with normal, hyperplasia, mPIN, and invasive adenocarcinoma in the ventral prostate (VP), dorsolateral prostate (DLSP), and anterior prostate (AP). (D) Number of mice of the indicated genotype that demonstrated a 4 + 4 Gleason score. (E) IHC staining intensities for NCAM1 and ASCL1 from prostates of mice of the indicated genotype. (F) Representative hematoxylin and eosin (H&E) and IHC sections from data shown above. Red arrowheads indicate cytoplasmic hyaline associated with atypia (VP). Results are mean ± SD from at least 10 mice, and multiple *t*-test was used for *p*-value determination. [Color figure can be viewed at wileyonlinelibrary.com]

4 | Discussion

Treatment approaches for advanced prostate cancer are impacted by the occurrence of NEPC. Spontaneous occurrence of NEPC is only 0.5%–2%; however, tNEPC is expected in 15%–30% of CRPC patients which will progress with increased drug potency [33–38]. Treatment-induced NEPC preserves CRPC genetic signatures (RB1/TP53/PTEN) alongside the emergence of NE-related gene expression [39–41]. These findings indicate a significant likelihood of impaired terminal differentiation originating from a CRPC precursor cell, rather than selection of a pre-existing NEPC subpopulation [42].

Previous studies report that long-term endocrine therapy can induce transcriptome reprogramming via epigenetic modulators [9]. PRMT5 is one of these regulators that plays a significant role in

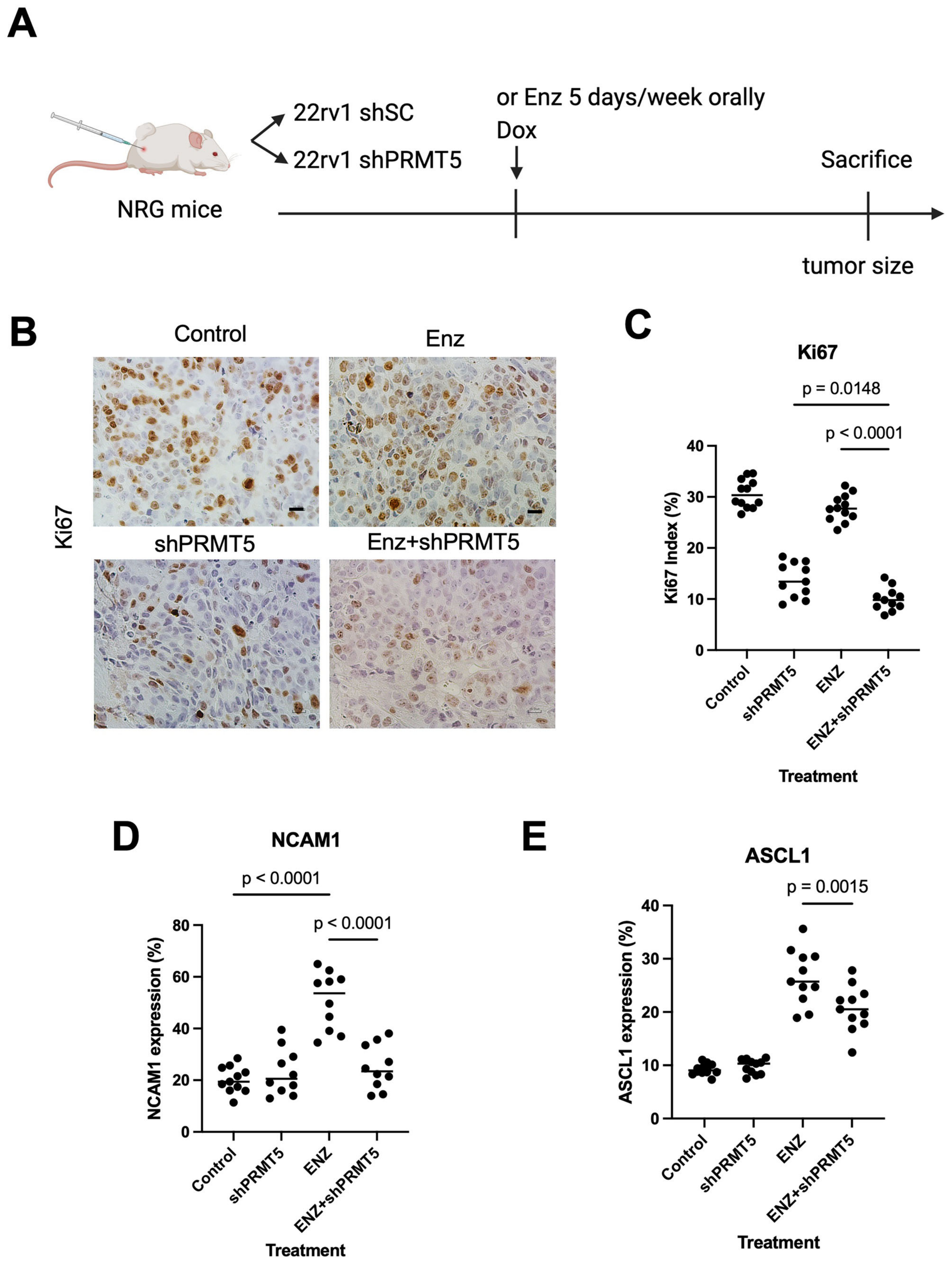

FIGURE 5 | Depletion of PRMT5 expression inhibits treatment-induced NED in vivo. (A) Schematic showing experimental timeline of 22Rv1 xenograft treated with enzalutamide. Created with Biorender.com. (B and C) Representative IHC images and quantification of Ki67 index (D and E) Quantification of NCAM1 and ASCL1 IHC staining from the indicated conditions. Results are the mean from at least five fields, and multiple *t*-test was used for *p*-value determination. [Color figure can be viewed at wileyonlinelibrary.com]

various cancers [20, 21, 43–45]. We previously reported that inhibition of PRMT5 can reduce CRPC cell growth and limit radiation-induced NED [24, 25]. In this study, we observe that PRMT5 and MEP50 gene expression is highly correlated with disease progression in prostate adenocarcinoma. Neuroendocrine prostate cancer is an aggressive subtype of disease, which indicates the potential of PRMT5:MEP50 as a predictive marker for future treatment. LNCaP cells can and have previously been cultured in the presence of DHT. However, we found that standard FBS is sufficient for these cells thrive in culture and produce an epithelial phenotype. Inhibition of androgen signaling through treating with ENZ or culturing in CBS-FBS resulted in an NED phenotype. Inhibition of PRMT5 expression or its activity successfully reduced NED and increased cell death induced by the AR inhibitor enzalutamide. Similar observations were made upon depletion of MEP50. These data explicitly show that both PRMT5 and MEP50 are required in the initiation and maintenance stages of drug induced NED.

Empowered by these observations, we sought to determine if overexpression of PRMT5:MEP50 would be sufficient to induce NED. Indeed, overexpression of PRMT5:MEP50 in androgen-dependent LNCaP cell line was coupled with induction and maintenance of NED. Use of a catalytically inactive form of PRMT5 or mutant of MEP50 that is incapable of interacting with PRMT5 failed to induce NED. In contrast to MEP50, co-expression of other known PRMT5 cofactors, pICln and RioK1, did not induce NED. To expand beyond in vitro models, we constructed a novel mouse model in which both PRMT5 and MEP50 are specifically overexpressed in mouse prostate. Analysis of this model further supported that PRMT5:MEP50 are not only sufficient to induce NED, but can also cause the initiation and progression of prostate hyperplasia. Taken together, these data indicate that the catalytic activity of PRMT5 while in physical interaction with MEP50 contributes to induction and maintenance of NEPC.

Our next goal was to assess the in vivo role of PRMT5 in enzalutamide-induced NED. Thus, we utilized a CRPC xenograft model to assess enzalutamide response in the absence of PRMT5. This approach similarly demonstrated that depletion of PRMT5 inhibited enzalutamide-induced NED.

Despite these promising findings, the limitation of the cell models raises the question of whether PRMT5:MEP50 co-overexpression-induced NED truly resembles ASI therapy-induced NED. Co-expression of PRMT5 and MEP50 may be sufficient to induce a NE-like morphology and enhance the expression of NE-related marker genes in prostate cancer cells; however, further investigation is required to understand how the PRMT5:MEP50 complex drives NED. Additionally, chromatin structure changes may disclose the epigenetic activities of PRMT5:MEP50 in NED. Further research identifying the overlap between accessible chromatin areas and differential gene expression might reveal the target genes involved in NED.

Author Contributions

Hye Seung Nam: conceptualization, methodology, validation, formal analysis, investigation, resources, data curation, writing – original draft, writing – review and editing. **Andrew Michael Asberry:** methodology, validation, investigation, writing – review and editing. **Xuehong Deng:** methodology, investigation, writing – review and editing. **Sheng Liu:** methodology, software, validation, formal analysis, investigation, resources, data curation, visualization, writing – review and editing. **Jiaoti Huang:** methodology, validation, formal analysis, resources. **Chang-Deng Hu:** conceptualization, methodology, validation, formal analysis, resources, data curation, writing – review and editing, supervision, project administration, funding acquisition. **Jun Wan:** conceptualization, methodology, software, validation, formal analysis, resources, data curation, writing – review and editing, supervision, project administration, funding acquisition. **Michael K. Wendt:** conceptualization, methodology, validation, formal analysis, resources, data curation, writing – review and editing, supervision, project administration, funding acquisition.

Acknowledgments

This study was supported by a grant from the Department of Defense (W81XWH2210332). We also acknowledge the support of the Purdue Institute for Cancer Research and the expertise of individuals its Biological Evaluation Core (P30CA023168). This work was partially supported by Indiana University Simon Comprehensive Cancer Center (IUSCCC, NIH/NCI P30CA082709), Walther Cancer Foundation, and the Near-Miss Initiative at IUSCCC. We also acknowledge the use of the facilities within the Bindley Bioscience Center, a core facility of the NIH-funded Indiana Clinical and Translational Sciences Institute. We acknowledge Purdue University College of Veterinary Medicine clinical pathology laboratory. This manuscript and work are dedicated to the life and legacy of our mentor, colleague, and friend, Dr. Chang-Deng Hu.

Conflicts of Interest

The authors declare no conflicts of interest.

Data Availability Statement

The data that support the findings of this study are openly available in Figshare at 10.6084/m9.figshare.29123255.v1.

References

1. *American Cancer Society: Cancer Facts & Figures 2003* (American Cancer Society, 2003).

2. S. You, B. S. Knudsen, N. Erho, et al., "Integrated Classification of Prostate Cancer Reveals a Novel Luminal Subtype With Poor Outcome," *Cancer Research* 76, no. 17 (2016): 4948–4958, https://doi.org/10.1158/0008-5472.CAN-16-0902.

3. C. Huggins and C. V. Hodges, "Studies on Prostatic Cancer: I The Effect of Castration, of Estrogen and of Androgen Injection on Serum Phosphatases in Metastatic Carcinoma of the Prostate," *CA: A Cancer Journal for Clinicians* 22, no. 4 (1972): 232–240, https://doi.org/10.3322/canjclin.22.4.232?sid=nlm%3Apubmed.

4. L. G. Gomella, "Effective Testosterone Suppression for Prostate Cancer: Is There a Best Castration Therapy?," *Reviews in Urology* 11, no. 2 (2009): 52–60.

5. I. D. Davis, A. J. Martin, and M. R. Stockler, "Enzalutamide with Standard First-Line Therapy in Metastatic Prostate Cancer," *New England Journal of Medicine* 381 (2024): 121–131, https://doi.org/10.1056/NEJMoa1903835.

6. C. Tran, S. Ouk, N. J. Clegg, et al., "Development of a Second-Generation Antiandrogen for Treatment of Advanced Prostate Cancer," *Science* 324, no. 5928 (2009): 787–790, https://doi.org/10.1126/science.1168175.

7. E. G. Bluemn, I. M. Coleman, J. M. Lucas, et al., "Androgen Receptor Pathway-Independent Prostate Cancer Is Sustained Through FGF Signaling," *Cancer Cell* 32, no. 4 (2017): 474–489.e6, https://pubmed.ncbi.nlm.nih.gov/29017058/.

8. H. T. Wang, Y. H. Yao, B. G. Li, et al., "Neuroendocrine Prostate Cancer (NEPC) Progressing From Conventional Prostatic Adenocarcinoma: Factors Associated With Time to Development of NEPC and Survival From NEPC Diagnosis-a Systematic Review and Pooled Analysis," *Journal of Clinical Oncology* 32, no. 30 (2014): 3383–3390, https://pubmed.ncbi.nlm.nih.gov/25225419/.

9. W. K. Storck, A. M. May, T. C. Westbrook, et al., "The Role of Epigenetic Change in Therapy-Induced Neuroendocrine Prostate Cancer Lineage Plasticity," *Frontiers in Endocrinology* 13 (2022): 926585, https://doi.org/10.3389/fendo.2022.926585.

10. H. Beltran, S. T. Tagawa, K. Park, et al., "Challenges in Recognizing Treatment-Related Neuroendocrine Prostate Cancer," *Journal of Clinical Oncology* 30, no. 36 (2012): e386–e389, https://pubmed.ncbi.nlm.nih.gov/23169519/.

11. V. Parimi, R. Goyal, K. Poropatich, and X. J. Yang, "Neuroendocrine Differentiation of Prostate Cancer: A Review," *American Journal of Clinical and Experimental Urology* 2, no. 4 (2014): 273–285.

12. J. Zhu, X. Liang, D. Wu, et al., "Clinicopathological Characteristics and Survival Outcomes in Neuroendocrine Prostate Cancer: A Population-Based Study," *Medicine* 100, no. 15 (2021): e25237, https://doi.org/10.1097/MD.0000000000025237.

13. S. Nouruzi, D. Ganguli, N. Tabrizian, et al., "ASCL1 Activates Neuronal Stem Cell-like Lineage Programming Through Remodeling of the Chromatin Landscape in Prostate Cancer," *Nature Communications* 13 (2022): 2282, https://www.nature.com/articles/s41467-022-29963-5.

14. J. L. Bishop, D. Thaper, S. Vahid, et al., "The Master Neural Transcription Factor BRN2 Is an Androgen Receptor–Suppressed Driver of Neuroendocrine Differentiation in Prostate Cancer," *Cancer Discovery* 7, no. 1 (2017): 54–71, https://doi.org/10.1158/2159-8290.CD-15-1263.

15. H. Chen, B. Lorton, V. Gupta, and D. Shechter, "A TGFβ-PRMT5-MEP50 Axis Regulates Cancer Cell Invasion Through Histone H3 and H4 Arginine Methylation Coupled Transcriptional Activation and Repression," *Oncogene* 36, no. 3 (2017): 373–386, https://doi.org/10.1038/onc.2016.205.

16. S. S. Tarighat, R. Santhanam, D. Frankhouser, et al., "The Dual Epigenetic Role of PRMT5 in Acute Myeloid Leukemia: Gene Activation and Repression via Histone Arginine Methylation," *Leukemia* 30, no. 4 (2016): 789–799, https://doi.org/10.1038/leu.2015.308.

17. M. C. Ho, C. Wilczek, J. B. Bonanno, et al., "Structure of the Arginine Methyltransferase PRMT5-MEP50 Reveals a Mechanism for Substrate Specificity," *PLoS One* 8, no. 2 (2013): e57008, https://doi.org/10.1371/JOURNAL.PONE.0057008.

18. G. Meister, C. Eggert, D. Bühler, H. Brahms, C. Kambach, and U. Fischer, "Methylation of Sm Proteins by a Complex Containing PRMT5 and the Putative U snRNP Assembly Factor pICln," *Current Biology* 11, no. 24 (2001): 1990–1994, https://doi.org/10.1016/S0960-9822(01)00592-9.

19. Q. Shen, Y. Liu, X. Deng, and C. D. Hu, "PRMT5promotes Chemotherapy-Induced Neuroendocrine Differentiation i78n NSCLC," *Thoracic Cancer* 14, no. 18 (2023): 1764–1773, https://doi.org/10.1111/1759-7714.14921.

20. E. Beketova, J. L. Owens, A. M. Asberry, and C. D. Hu, "PRMT5: a Putative Oncogene and Therapeutic Target in Prostate Cancer," *Cancer Gene Therapy* 29, no. 3–4 (2022): 264–276, https://doi.org/10.1038/s41417-021-00327-3.

21. Z. Mounir, J. M. Korn, T. Westerling, et al., "ERG Signaling in Prostate Cancer Is Driven Through PRMT5-Dependent Methylation of the Androgen Receptor," *eLife* 5 (2016): e13964, https://doi.org/10.7554/eLife.13964.

22. X. Deng, G. Shao, H. T. Zhang, et al., "Protein Arginine Methyltransferase 5 Functions as an Epigenetic Activator of the Androgen Receptor to Promote Prostate Cancer Cell Growth," *Oncogene* 36, no. 9 (2017): 1223–1231, https://doi.org/10.1038/onc.2016.287.

23. J. L. Owens, E. Beketova, S. Liu, et al., "PRMT5 Cooperates With pICln to Function as a Master Epigenetic Activator of DNA Double-Strand Break Repair Genes," *iScience* 23, no. 1 (2020): 100750, https://doi.org/10.1016/j.isci.2019.100750.

24. E. Beketova, S. Fang, J. L. Owens, et al., "Protein Arginine Methyltransferase 5 Promotes pICln-Dependent Androgen Receptor Transcription in Castration-Resistant Prostate Cancer," *Cancer Research* 80, no. 22 (2020): 4904–4917, https://doi.org/10.1158/0008-5472.CAN-20-1228.

25. J. L. Owens, E. Beketova, S. Liu, et al., "Targeting Protein Arginine Methyltransferase 5 Suppresses Radiation-Induced Neuroendocrine Differentiation and Sensitizes Prostate Cancer Cells to Radiation," *Molecular Cancer Therapeutics* 21, no. 3 (2022): 448–459, https://doi.org/10.1158/1535-7163.MCT-21-0103.

26. J. H. Park, M. Szemes, G. C. Vieira, et al., "Protein Arginine Methyltransferase 5 Is a Key Regulator of the MYCN Oncoprote in Neuroblastoma Cells," *Molecular oncology* 9, no. 3 (2015): 617–627, https://doi.org/10.1016/j.molonc.2014.10.015.

27. A. Scoumanne, J. Zhang, and X. Chen, "PRMT5 Is Required for Cell-Cycle Progression and p53 Tumor Suppressor Function," *Nucleic Acids Research* 37, no. 15 (2009): 4965–4976, https://doi.org/10.1093/nar/gkp516.

28. M. Jansson, S. T. Durant, E.-C. Cho, et al., "Arginine Methylation Regulates the p53 Response," *Nature Cell Biology* 10 (2008): 1431, https://www.nature.com/articles/ncb1802.

29. Y. K. Banasavadi-Siddegowda, L. Russell, E. Frair, et al., "PRMT5-PTEN Molecular Pathway Regulates Senescence and Self-Renewal of Primary Glioblastoma Neurosphere Cells," *Oncogene* 36, no. 2 (2017): 263–274, https://doi.org/10.1038/onc.2016.199.

30. L. Wang, S. Pal, and S. Sif, "Protein Arginine Methyltransferase 5 Suppresses the Transcription of the RB Family of Tumor Suppressors in Leukemia and Lymphoma Cells," *Molecular and Cellular Biology* 28, no. 20 (2008): 6262–6277, https://doi.org/10.1128/MCB.00923-08.

31. B. P. Pollack, S. V. Kotenko, W. He, L. S. Izotova, B. L. Barnoski, and S. Pestka, "The Human Homologue of the Yeast Proteins Skb1 and Hsl7p Interacts With Jak Kinases and Contains Protein Methyltransferase Activity," *Journal of Biological Chemistry* 274 (1999): 31531–31542, https://doi.org/10.1074/jbc.274.44.31531.

32. A. M. Asberry, X. Cai, X. Deng, et al., "Discovery and Biological Characterization of PRMT5:MEP50 Protein-Protein Interaction Inhibitors," *Journal of Medicinal Chemistry* 65, no. 20 (2022): 13793–13812, https://doi.org/10.1021/acs.jmedchem.2c01000.

33. M. F. Sarosdy, "Which Is the Optimal Antiandrogen for Use in Combined Androgen Blockade of Advanced Prostate Cancer? The Transition From a First- to Second-Generation Antiandrogen," *Anti-Cancer Drugs* 10, no. 9 (1999): 791–796, https://doi.org/10.1097/00001813-199910000-00001.

34. M. R. Smith, M. Hussain, F. Saad, et al., "Darolutamide and Survival in Metastatic, Hormone-Sensitive Prostate Cancer," *New England Journal of Medicine* 386, no. 12 (2022): 1132–1142, https://doi.org/10.1056/NEJMoa2119115.

35. M. Hussain, K. Fizazi, N. D. Shore, et al., "Metastatic Hormone-Sensitive Prostate Cancer and Combination Treatment Outcomes: A Review," *JAMA Oncology* 10, no. 6 (2024): 807–820, https://doi.org/10.1001/jamaoncol.2024.0591.

36. T. M. Beer, A. J. Armstrong, D. E. Rathkopf, et al., "Enzalutamide in Metastatic Prostate Cancer before Chemotherapy," *New England Journal of Medicine* 371, no. 5 (2014): 424–433, https://doi.org/10.1056/NEJMoa1405095.

37. N. D. Shore, S. Chowdhury, A. Villers, et al., "Efficacy and Safety of Enzalutamide Versus Bicalutamide for Patients With Metastatic Prostate Cancer (TERRAIN): A Randomised, Double-Blind, Phase 2 Study,"

Lancet Oncology 17, no. 2 (2016): 153–163, https://doi.org/10.1016/S1470-2045(15)00518-5.

38. D. L. Suzman, B. Luber, M. T. Schweizer, R. Nadal, and E. S. Antonarakis, "Clinical Activity of Enzalutamide Versus Docetaxel in Men With Castration-Resistant Prostate Cancer Progressing After Abiraterone," *Prostate* 74, no. 13 (2014): 1278–1285, https://doi.org/10.1002/pros.22844.

39. S. Y. Ku, S. Rosario, Y. Wang, et al., "Rb1 and Trp53 Cooperate to Suppress Prostate Cancer Lineage Plasticity, Metastasis, and Antiandrogen Resistance," *Science* 355, no. 6320 (2017): 78–83, https://doi.org/10.1126/science.aah4199.

40. M. G. Velez, H. E. Kosiorek, J. B. Egan, et al., "Differential Impact of Tumor Suppressor Gene (TP53, PTEN, RB1) Alterations and Treatment Outcomes in Metastatic, Hormone-Sensitive Prostate Cancer," *Prostate Cancer and Prostatic Diseases* 25 (2021): 479–483, https://www.nature.com/articles/s41391-021-00430-4.

41. M. D. Nyquist, A. Corella, I. Coleman, et al., "Combined *TP53* and *RB1* Loss Promotes Prostate Cancer Resistance to a Spectrum of Therapeutics and Confers Vulnerability to Replication Stress," *Cell Reports* 31, no. 8 (2020): 107669, https://doi.org/10.1016/j.celrep.2020.107669.

42. L. Puca, P. J. Vlachostergios, and H. Beltran, "Neuroendocrine Differentiation in Prostate Cancer: Emerging Biology, Models, and Therapies," *Cold Spring Harbor Perspectives in Medicine* 9, no. 2 (2019): a030593, https://doi.org/10.1101/cshperspect.a030593.

43. S. L. Sloan, F. Brown, M. Long, et al., "PRMT5 Supports Multiple Oncogenic Pathways in Mantle Cell Lymphoma," *Blood* 142, no. 10 (2023): 887–902, https://doi.org/10.1182/blood.2022019419.

44. C. C. Lin, T. C. Chang, Y. Wang, et al., "PRMT5 Is an Actionable Therapeutic Target in CDK4/6 Inhibitor-ResistantER+/RB-Deficient Breast Cancer," *Nature Communications* 15, no. 1 (2024): 2287, https://doi.org/10.1038/s41467-024-46495-2.

45. H. Kim and Z. A. Ronai, "PRMT5 Function and Targeting in Cancer," *Cell Stress* 4, no. 8 (2020): 199–215, https://doi.org/10.15698/cst2020.08.228.

Supporting Information

Additional supporting information can be found online in the Supporting Information section.